**University of Szeged**
**Doctoral School of Pharmaceutical Sciences**

Pharmacodynamics, biopharmacy, clinical pharmacy **Ph.D. programme**
**Programme director:** István Zupkó Ph.D., D.Sc.

**Department of Pharmacodynamics and Biopharmacy**
**Supervisor:** István Zupkó Ph.D, D.Sc.

**Ágnes Erika Kulmány Pharm.D.**

# Characterization of antiproliferative and antimetastatic properties of novel androstane derivatives

**Final Exam Committee:**

Chairman: Gyöngyvér Soós Ph.D.
Committee members: Eszter Ducza Ph.D.
László Puskás Ph.D., D.Sc.

**Reviewer Committee:**

Chairman: Zsolt Szakonyi Ph.D., D.Sc.
Official reviewers: Gábor Halmos Ph.D.
Gabriella Spengler Ph.D.
Committee members: Gerda Szakonyi Ph.D.
Dóra Rédei Ph.D.

**2021**

# 1. Introduction

Cancer represents one of the major health burdens and a leading cause of mortality worldwide, responsible for millions of deaths annually. The latest survey of the Global Cancer Observatory (GLOBOCAN) series – published by International Agency for Research on Cancer (IARC) – estimated 19.3 million new cancer cases and 9.6 million cancer-related deaths in 2020. Among females, breast cancer is the most frequently diagnosed type and the principal cause of cancer-related deaths, responsible for 2.26 million new cases and 685,000 deaths, while cervical neoplasms are the fourth most common, both in incidence and mortality, with approximately 604,000 new cases and 342,000 deaths. Although a very high proportion of cancer cases may be treated successfully with improved survival outcome by early diagnosis (owning to milder symptoms or asymptomatic characteristic of the early stages), due to the lack of resources and protocols in many countries, neoplasms are often identified only in their advanced stages. Moreover, success of the therapy is limited by *de novo* or acquired resistance against anticancer drugs. Besides rapid advancement in preventive, diagnostic and therapeutic strategies, in the light of previously described facts, novel treatment options of breast and cervical tumors are eagerly awaited.

Biologically active molecules with a steroidal framework constitute a diverse and extensive group of organic compounds. Hundreds of natural derivatives are found in plants, fungi and animals, while preparation of semisynthetic or synthetic analogues is one of the prominent fields of pharmaceutical research. Sexual steroids (estrogens, progestogens and androgens) are essential parts of human hormonal system. Plenty of these compounds, as well as their semi-synthetic and synthetic derivatives, are used for therapeutic purposes, including anabolics, hormonal contraceptives or as part of hormone replacement therapy. Besides their physiological impacts, sexual steroids are also involved in the development of numerous hormone-dependent malignancies, such as prostate, breast, endometrial cancer or hormone-independent types, e.g., bladder, lung, colorectal and brain tumors as well. Recent studies suggest that some natural androstanes, as well as their A- or D-ring modified derivatives are able to inhibit proliferation of breast or gynaecological cancer cells, induce cell cycle disruptions and have proapoptotic, antimigratory and antimetastatic properties, without hormonal or antihormonal characteristic. Comprehensive analysis of structure-activity relationships proved that the incorporation of bulky heterocyclic moiety on the D-ring may result in promising anticancer drug candidates without hormonal activity.

## 2. Aims

During our experiments, four novel, heterocyclic, D-ring modified androstane derivatives were examined. 3β-Hydroxy-17-[1'-(4''-cyanophenyl)-4'-hydroxymethyl-1'H-pyrazol-3'-yl]androsta-5,16-diene exerted pronounced antiproliferative properties on breast cancer cell lines as reported previously.[55] The aim of the present study was to examine the antiproliferative and antimetastatic characteristics and the underlying mechanism of action of these promising compounds with *in vitro* and *in vivo* experiments on breast and gynaecological tumor cell lines.

The purposes of the performed experiments were as follows:

- Caracterization of antiproliferative properties of the tested compounds on breast and gynaecological cancer cell lines, and the determination of their $IC_{50}$ values by standard MTT assay.

- Estimation of tumor selectivity indices on all of the investigated cell lines compared to a non-cancerous cell line (NIH/3T3).

- Detection of apoptosis-inducing effects of the tested compounds, and their pathway using Hoechst/propidium iodide and Annexin V/propidium iodide fluorescent double staining methods, cell cycle analysis, colorimetric determination of caspase-3 activity and mitochondrial membrane potential assay (JC-1 assay).

- Demonstrating the possible androgenic/antiandrogenic activity of the tested compounds, owing to the androstane skeleton by yeast androgen screening assay (YAS).

- Examination of the inhibitory effects of the tested compounds to the early steps of metastasis formation such as migration, invasion and intravasation, carrying out wound-healing, Boyden chamber and circular chemorepellent-induced defects (CCIDs) assays.

- Analysis of expression level of tumor markers upon treatment with the tested compounds.

- Investigation of *in vivo* administration of the tested compounds on the 4T1 ortothopic mouse breast cancer model.

# 3. Materials and methods

## 3.1 Chemicals

Synthesis and chemical characterization of the test compounds were carried out by Éva Frank *et al.* as reported previously or by the colleagues of the Department of Chemistry, Biochemistry and Environmental Protection, University of Novi Sad, Serbia.
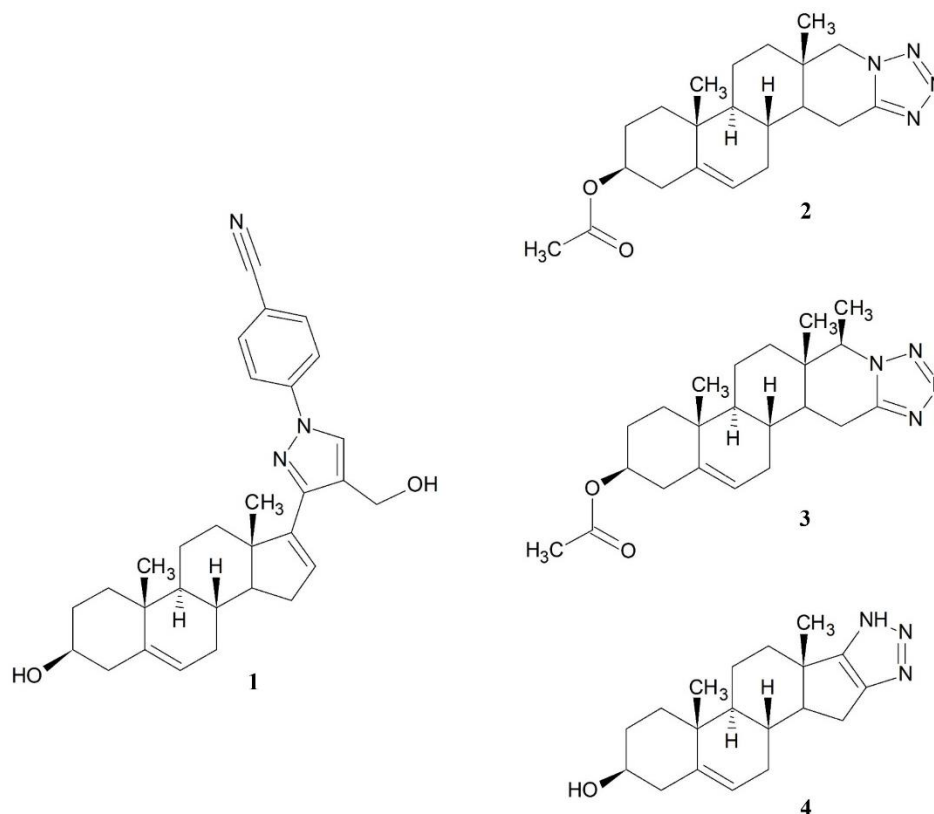


**Figure 1.** Chemical structures of the tested compounds (**1-4**).

## 3.2 Cell lines

HeLa, SiHa, C33A, A2780, MCF-7, T-47D, MDA-MB-231 and NIH/3T3 cells were maintained in Eagle's Minimal Essential Medium (EMEM), supplemented with 10% fetal bovine serum (FBS), 1% non-essential amino acid (NEAA) mixture and 1% penicillin, streptomycin and amphotericin B mixture at 37°C in a humidified carbon dioxide ($CO_2$) atmosphere. iLEC cells were grown in EGM-2MV medium under the same conditions. MDA-MB-361 cells were cultivated in L-15 medium, complemented with 20% FBS, 1% NEAA mixture and 1% antibiotic/antimicotic mixture at 37 °C, under humidified carbon dioxide-free circumstances. 4T1 mouse breast cancer cells were cultured in RPMI medium containing 10% FBS, 1% NEAA mixture and 1% antibiotic solution in $CO_2$ incubator at 37°C.

## 3.3 MTT-assay (antiproliferative assay)

Proliferation and viability of cells upon treatment with the test compounds were investigated by the standard MTT assay. All cell types were maintained under the cell culturing circumstances described previously, and were seeded into 96-well plates and were treated with increasing concentrations of the test substances (0.1-30 µM). After 72 h of incubation, MTT solution was added to the wells for 4 h and the precipitated, blue formazan crystals were dissolved in DMSO. Finally, absorbance values were recorded by a microplate reader at 545 nm and normalized six-point dose-response curves were evaluated by GraphPad Prism 5.01 software.

## 3.4 Hoechst/Propidium iodide fluorescent double staining

Apoptosis or necrosis-related changes in cell morphology and membrane integrity were investigated by Hoechst 33258 and propidium iodide (PI) fluorescent staining. Suspension of MCF-7 and SiHa cells were seeded into 96-well plates and were treated with increasing concentrations of compound **1** for 24 h. After treatment period, cells were stained in the dark, under cell culturing conditions described above for 1 hour and images were taken by the QCapture Pro software and a Nikon Eclipse TS100 fluorescence microscope. Nuclei emitting fluorescence were counted and the proportion of intact, apoptotic and necrotic cell populations were expressed as percentages.

## 3.5 Apoptosis Assay

MCF-7, MDA-MB-231, SiHa and C33A cells were seeded into 24 well cell culture plates and were treated with different concentrations of the test compound (**1**) for 24 h. Next, cells were washed with phosphate-buffered saline (PBS), harvested with trypsin and pooled with the collected supernatants. Samples were centrifuged and pellets were resuspended in Annexin V binding buffer accompanied by staining procedure with Annexin V-Alexa488 and PI solution in the dark at room temperature for 15 minutes. For each sample, 10 000 events were detected by FACSCalibur cytofluorimeter and data were analysed by CellQuest™ software.

### 3.6 Cell cycle analysis

Briefly, MCF-7, MDA-MB-231, SiHa and C33A cells were seeded onto 24-well plates and were exposed to our drug candidate (**1**) for 48 h or 72 h. The samples were washed with PBS, collected, pooled with the corresponding supernatants and centrifuged. The DNA content of resuspended cells were labelled with PI in DNA staining solution in the dark, at room temperature for 30 min. Analysis of at least 20,000 events/sample were carried out by the FACSCalibur flow cytometer and the Kaluza Analysis software.

### 3.7 Determination of caspase-3 activity

SiHa cells were grown in cell culture flasks under standard cell culturing conditions and treated for 24, 48 and 72 h. Thereafter, cells were collected with a special cell scraper tool and counted. Samples were centrifuged, supernatants were gently removed and cells were lysated by required amount of lysis buffer of the kit on ice for 20 min. Next, lysates were centrifuged and 5 µL portions of the supernatants were incubated overnight with 10 µL substrate (acetyl-Asp-Glu-Val-Asp-p-nitroanilide) and assay buffer in 96-well plate at 37°C according to the manufacturer's protocol. Finally, absorbance values of the colorful substrate cleaved by caspase-3 in samples were detected at 405 nm with a microplate reader.

### 3.8 Mitochondrial membrane potential assay (JC-1 staining)

MCF-7, MDA-MB-231, SiHa and C33A cells were grown and harvested under standard cell culturing conditions, and were seeded onto 24-well plates. After 12 h (MCF-7, MDA-MB-231) or 24 h (SiHa, C33A) treatment of compound **1**, samples were washed, collected and centrifuged. After that, pellets were resuspended and stained with JC-1 solution (5 µg/ml) at 37°C for 5 minutes. Finally, red and green fluorescence of the cells were investigated on FL2 (585/42 nm) - FL1 (530/30 nm) channels by the FACSCalibur flow cytometer.

### 3.9 Yeast Androgen Screen assay (YAS)

The yeast cells were grown in humidified air at 31°C on an orbital shaker. Next, they were plated onto assay plates and were incubated in the presence of the CPRG substrate and the test substance and/or 5α-dihydrotestosterone (DHT) used as reference agent, for 2 days. Androgenic activity triggers the expression of β-galactosidase from the reporter gene and this enzyme can convert the yellow CPRG substrate into a red product. Absorbance of samples were detected at 570 nm and 690 nm.

## 3.10 Wound-healing assay

In our experiments, MCF-7 and SiHa cells were implanted in special silicon inserts, which were placed onto 24-well plates, in standard EMEM medium, containing 10% FBS. After overnight incubation, inserts were removed cautiously and the confluent monolayers with certain cell-free areas were washed with PBS. Cells were treated with sub-antiproliferative concentrations of compound **1** in EMEM medium containing 2% FBS, and images were taken by a Nikon Eclipse TS100 microscope 0, 24 and 48 h post-treatment.

## 3.11 Boyden chamber assay

After prehydration of a polyethylene terephthalate (PET) membrane in special Boyden chamber inserts placed onto a 24-well plate, cell suspension prepared in serum-free EMEM with sub-antiproliferative concentrations of the test substance (**1**) was nested in the upper compartments and EMEM medium supplemented with 10% FBS was applied as a chemoattractant in the lower chambers. After 24 h incubation, invading cells were fixed in ice cold 96% ethanol and were stained by 1% crystal violet dye. Images were taken by the Nikon Eclipse TS100 microscope and the number of invading cells was counted.

## 3.12 Circular chemorepellent-induced defects assay (CCIDs)

Initially, MCF-7 cells suspended in EMEM medium, complemented with a methylcellulose solution were plated onto U-bottom 96-well plates, centrifuged and incubated for 3 days to form spheroids. Non-cancerous human lymphatic endothelial cells (iLEC) were seeded onto 24-well plates and grown to approximately 100% of confluency. Before measurement, iLEC monolayers were stained with CellTracker Green dye. The endothelial barriers and selected tumor spheroids were pre-incubated with compound **1** or defactinib or epiandrosterone for 20 minutes, separately. After pretreatment, the spheroids were placed upon the iLEC cell monolayer and incubated in the presence of the test compounds for 4 hours. Finally, images of at least 12 spheroids per condition were taken by fluorescent Axiovert microscope.

## 3.13 Single cell mass cytometry

Briefly, MDA-MB-231 cells were seeded and were incubated with compound **1** for 72 h. After treatment, cells were washed, collected and were centrifuged. Pellets were suspended in PBS and cells were counted. To demonstrate viability of the cells, cisplatin staining was

carried out on ice for 3 min. Samples were diluted with Maxpar Cell Staining Buffer (MCSB), centrifuged and were incubated with TruStain FcX, to prevent non-specific binding of the antibodies. Samples were centrifuged, suspended and the resultant antibody mix was added to fresh master pool of antibodies. After 60 min of incubation at 4°C, the cells were washed and centrifuged, and the pellets were re-suspended in the residual volume. Fixation of the samples was accomplished in 1.6% formaldehyde. Next, the cells were centrifuged, and the Cell-ID DNA intercalator was added to the samples for overnight incubation. After additional washing steps, the samples were centrifuged and the pellets were suspended in 1 mL PBS. For the measurement, the cell number was set in a cell acquisition solution, containing 10% EQ Calibration Beads and the samples were percolated with gravity filter. After manual gating singlets were analysed by the Cytobank platform.

## 3.14 *In vivo* mouse model of breast cancer

BALB/c mice were housed in sterile, IVC cage system, equipped with a HEPA filter at ambient temperature of 25°C. At the first day of the experiment, 4T1 breast carcinoma cells suspended in FBS-free RPMI medium, were injected into the mammary pad of the mice. On the 12th day of the experiment, animals were randomized into two groups. Members of the test group were treated intraperitoneally with 25 mg/kg dose of compound **1**, dissolved in mixture of DMSO : Solutol HS 15 : saline (1:3:10) once per day, five times per week for 2 weeks. Animals of the control group were treated with the vehicle mixture. Tumor size and body mass were determined daily, and on the 15th day of treatment period, animals were terminated. Finally, weight of the surgically removed tumor tissues were measured.

## 3.15 Statistical analysis

For statistical analyses, GraphPad Prism version 5.01 software was used. The statistical significance was estimated by one-way analysis of variance (ANOVA), followed by the Dunnett post-test. In the Results section, all data are presented as means ± SEM of at least three replicates. *, ** and *** indicate $p<0.05$, $p<0.01$ and $p< 0.001$ compared to control samples, respectively.

# 4. Results

## 4.1 MTT assay

Compound **1** exerted considerable antiproliferative activity against breast and cervical cancer cell lines, while compound **2**, **3** and **4** showed no substantial effect on cell proliferation; thus, compound **1** was selected for further experimentation. For comparison, the $IC_{50}$ values of therapeutically applied cisplatin used as reference agent, are presented for the same cell lines.

| Cell line | Calculated $IC_{50}$ value (µM) | | | | |
|-----------|----------|------|------|-------|--------|
| Compound | **1** | **2** | **3** | **4** | **CIS** |
| **HeLa** | 1.13 | >30 | >30 | >30 | 13.75 |
| **SiHa** | 0.78 | >30 | >30 | >30 | 13.51 |
| **C33A** | 1.72 | >30 | >30 | >30 | 3.09 |
| **A2780** | 2.34 | >30 | >30 | 29.58 | 1.30# |
| **MCF-7** | 1.40* | >30 | >30 | >30 | 5.78# |
| **T47D** | 1.20* | >30 | >30 | >30 | 9.78# |
| **MDA-MB-361** | 1.60* | >30 | >30 | >30 | 3.74# |
| **MDA-MB-231** | 1.80* | >30 | >30 | >30 | 19.13# |

**Table 1.** Calculated $IC_{50}$ values of compound **1-4** and cisplatin (**CIS**) determined on eight human breast- or gynaecological cancer cell lines. * and # are data from literature

In order to obtain information about tumor-selectivity, quotients of $IC_{50}$ values determined on cancerous and non-cancerous (NIH/3T3) cells were prepared. In case of compound **1**, these tumor selectivity indices were <1 but >0.1, which indicate moderate selectivity.

## 4.2 Hoechst/Propidium iodide fluorescent double staining

Changes in cell morphology and the membrane integrity of MCF-7 and SiHa cells were observed 24 h post-treatment. Fluorescent images revealed decreased number of viable cells, and significant elevation in the number of nuclei emitting light blue fluorescence due to DNA condensation in early apoptosis and red fluorescence in secondary necrotic cells with damaged cell membrane in a concentration-dependent manner.

## 4.3 Apoptosis assay

In all cancer cell lines, compound **1** triggered a concentration-dependent elevation of phosphatidylserine exposure as an indicator of apoptotic process (early apoptosis: AnnV+/PI−; late apoptosis: AnnV+/PI+) without presence of massive necrotic cell population (necrosis: AnnV−/PI+).
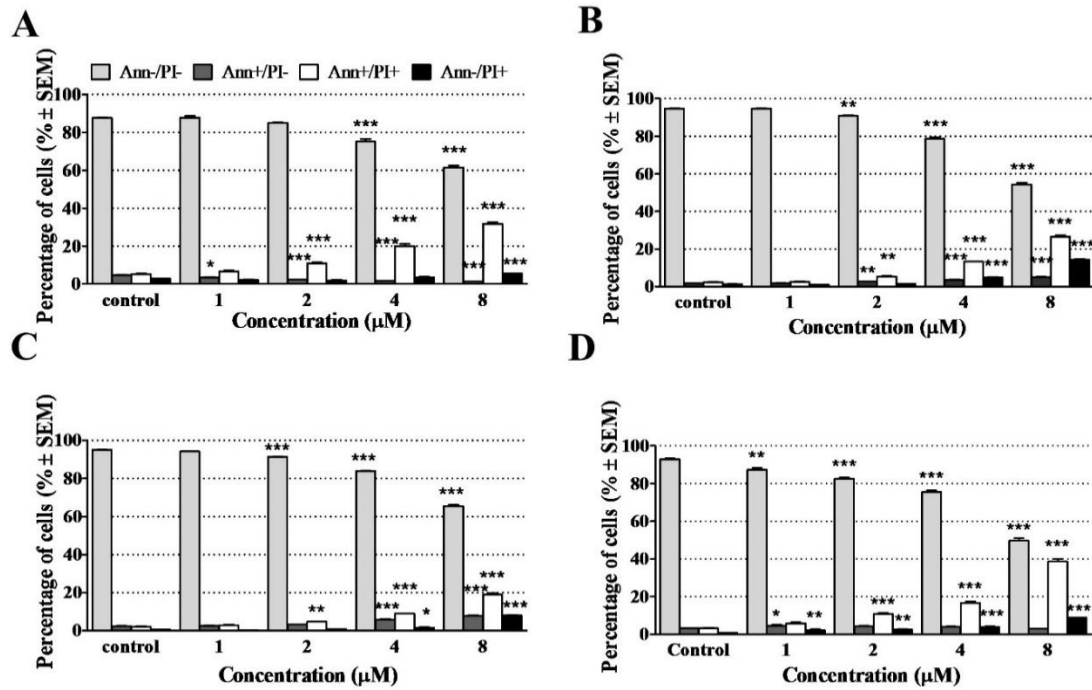
**Figure 2.** Compound **1** induced accumulation of early and/or late apoptotic cell populations. Changes in intact (AnnV–/PI–), early apoptotic (AnnV+/PI–), late apoptotic (AnnV+/PI+), and necrotic (AnnV–/PI+) populations of MCF-7 (A), MDA-MB-231 (B), SiHa (C) and C33A (D) cells are presented in percentage. *, ** and *** indicate $p < 0.05$, $p < 0.01$ and $p < 0.001$, respectively.
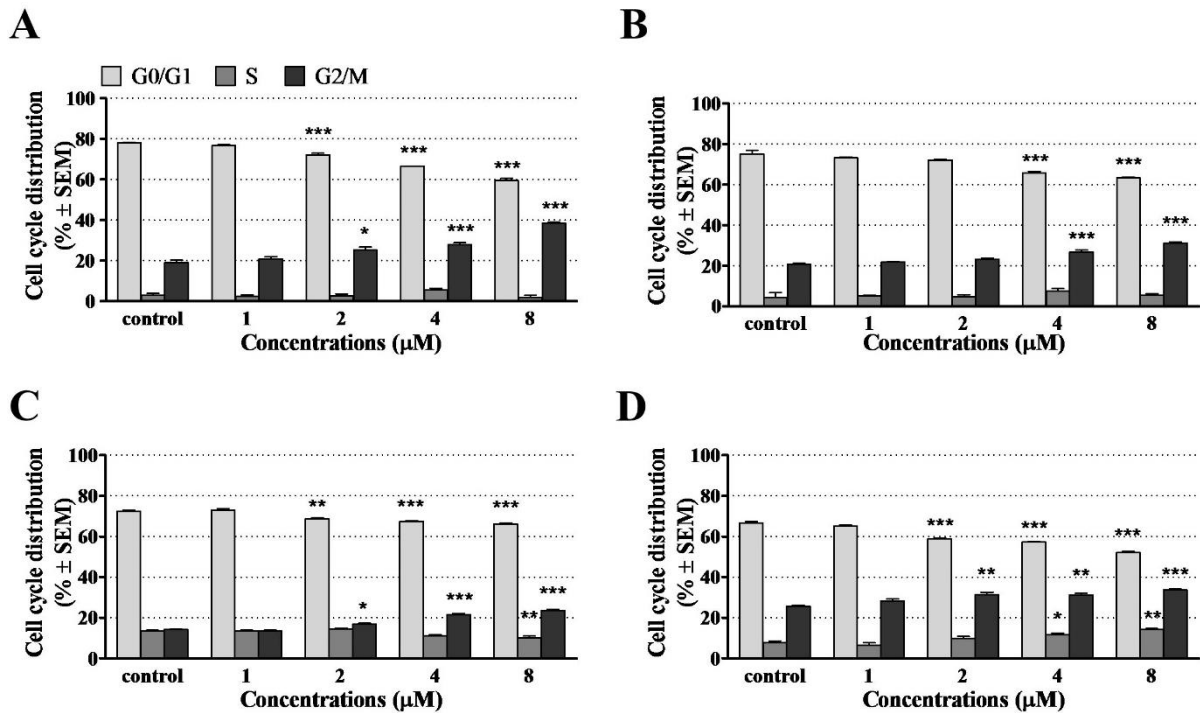
## 4.4 Cell cycle analysis



**Figure 3.** Test compound **1** induced cell cycle disturbances via accumulation of cells in the G2/M phase and reduction of the G0/G1 phase. Experiments were carried out on MCF-7 (A), SiHa (C) and C33A

(D) cell lines 48 h post-treatment, while in the case of triple negative breast cancer cell line (B), 72 h incubation time showed favourable effect. *, ** and *** indicate $p < 0.05$, $p < 0.01$ and $p < 0.001$ respectively, compared to the untreated control.

Concentration-dependent elevation of hypodiploid sub-G1 population, regarded as marker of apoptotic process, were recorded at $\geq 2$ $\mu$M in all of the four examined cell lines (MCF-7, MDA-MB-231, SiHa, C33A) after 48 h treatment. Besides these findings, significant accumulation of cells in G2/M phase to the detriment of G0/G1 phase were observed in all examined malignant cell lines.

## 4.5 Determination of caspase-3 activity

The androstadiene analogue (**1**) enhanced the caspase-3 activity by 1.6 to 2.6-fold after 24, 48 and 72 h exposure at $\geq 2$ $\mu$M concentrations on the SiHa cell line.

## 4.6 Mitochondrial membrane potential assay (JC-1 staining)

In MCF-7, MDA-MB-231, SiHa and C33A samples stained by JC-1 dye, a concentration-dependent elevation in the percentage of subpopulations emitting green fluorescence were detected.
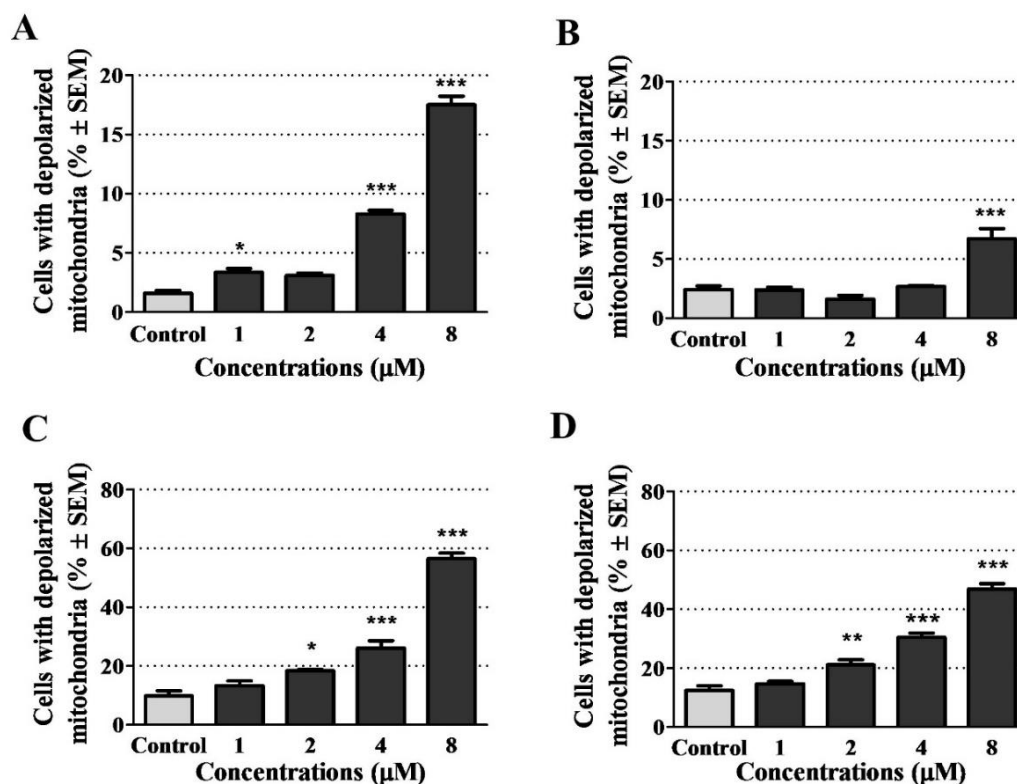


**Figure 4.** Considerable, concentration-dependent alterations in mitochondrial membrane integrity were observed in MCF-7 (A) and MDA-MB-231 cells (B) 12 h post-treatment and in SiHa (C) and C33A (D)

cells after 24 h incubation with the test substance (**1**). *, ** and *** represent $p<0.05$, $p<0.01$ and $p<0.001$ respectively, compared to the control.

## 4.7 Yeast androgen screen assay (YAS)

In the presence of an androgen-sensitive, genetically modified yeast strain (*S. cerevisiae*), no substantial androgenic or antiandrogenic activity of compound **1** were identified compared to DHT in the agonistic and to flutamide in antagonistic determination, used as reference agents after 48 h exposure.

## 4.8 Wound-healing assay

Image analysis confirmed noteworthy decrease in migratory capacity of MCF-7 cells by 30.8% and 22.8% at 0.3 µM compared to control after 24 or 48 h treatment. Similarly, influence of compound **1** to migration of SiHa cells manifested in a significant reduction of wound-closure by 9.0% and 21.7% at 0.03 µM 24 h or 48 h post-treatment, respectively.

## 4.9 Boyden chamber assay

In this system, the number of invading MDA-MB-231 triple negative breast cancer cells were decreased by approximately 70% at 0.3 µM. Furthermore, number of invading cervical SiHa cells were significantly diminished by 48.9% after application of 0.03 µM of compound **1** for 24 h.
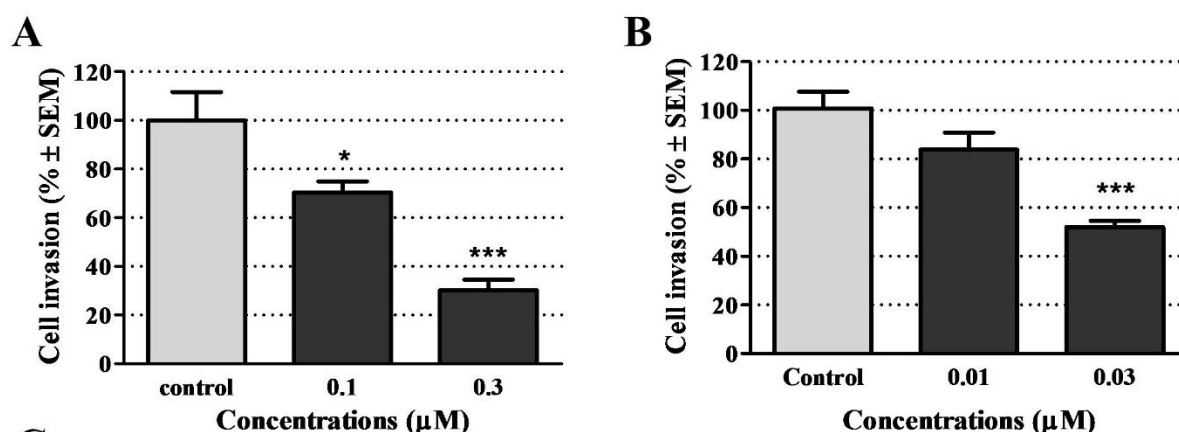


**Figure 5**. Anti-invasive properties of the test substance (**1**) were demonstrated by considerable decrease in percentage of invading MDA-MB-231 (A) and SiHa (B) cells in the treated samples compared to untreated control 24 h post-treatment. * and *** represent $p<0.05$ and $p<0.001$ respectively.

## 4.10 CCIDs assay

Cancer spheroids – consisting of MCF-7 cells – induced gap-formation in the monolayer of iLEC cells; this process was significantly inhibited by treatment with compound **1** or defactinib, which served as positive control. However, the structurally-similar epiandrosterone, only exerted a minor anti-invasive effect at 40 µM.
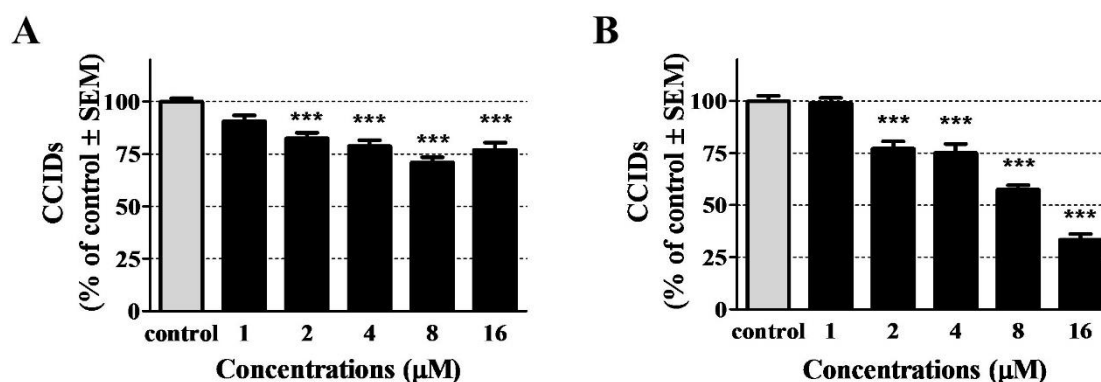


**Figure 6.** Our test substance (A) and defactinib (B) decreased size of cell-free areas at 2 µM 4 h post-treatment. *** indicates p<0.001 compared to the control.

## 4.11 Single Cell Mass Cytometry

To characterize the tumor marker profile of chemosensitive subpopulations of the MDA-MB-231 cell line, nine carcinoma markers were investigated at single cell resolution. Substantial decrease was detected in the percentage of cells positive for EGFR, CD274 (PD-L1), and CD326 (EpCAM) within the drug-sensitive population upon the treatment of compound **1**. On the other hand, elevated expression levels of GLUT1, MCT4, Pan-Keratin, CD66 (a,c,e), Gal-3 and TMEM45A were observed in the chemosensitive populations.

## 4.12 *In vivo* mouse breast cancer model

After 2 weeks of intraperitoneal administration of 25 mg/kg dose, a significant reduction in weight of the induced tumor tissues was observed. In addition, noteworthy deceleration in tumor growth rate was revealed in the treated group from the fourth day of the application period, compared to the control animals without provoking of severe, life-threatening side effects.
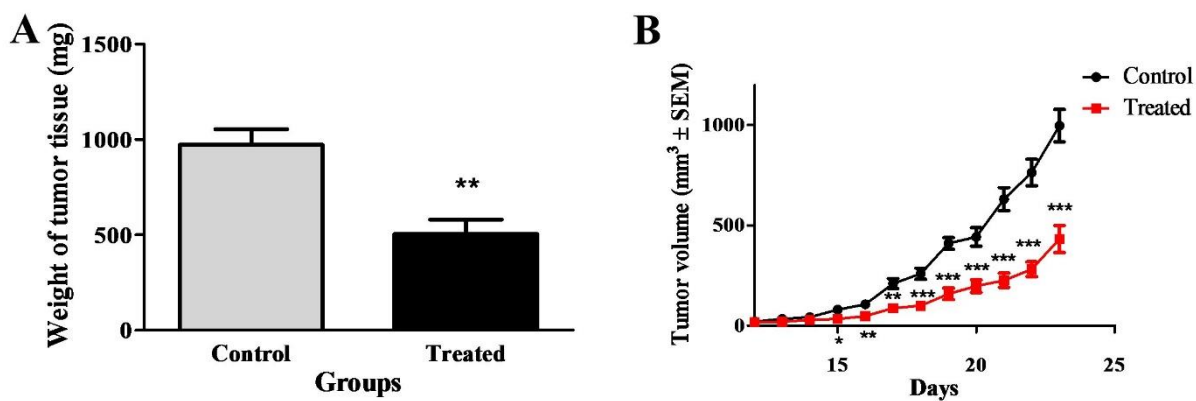
**Figure 7.** After 14 days of intraperitoneal application, the mean weight of surgically removed tumor tissues (n=7) was considerable decreased in the experimental group (A). Tumor growth curves (B) demonstrate a significant tumor growth inhibitory effect of compound **1** *in vivo*. *, ** and *** indicate $p<0.05$, $p<0.01$ and $p<0.001$ respectively, compared to the control.

# 5. Discussion

In the human body, sexual steroids exhibit great impact on cell proliferation, but precisely because of this, they may also be responsible for the development and progression of several hormone-dependent malignancies, such as breast or prostate cancer. On the other hand, modification of their structure at relevant positions, especially on the A- and/or D-ring, may yield novel anticancer agents. The aim of the present study was to evaluate the pharmacological potential of four D-ring modified androstane derivatives, with special regard to their antiproliferative and antimetastatic properties on breast and gynaecological cancer cells.

The antiproliferative effect of compound **2**, **3** and **4** did not reach the threshold of at least 50% of inhibition at 30 µM concentration in most of the cases. $IC_{50}$ values of the candidate compound (**1**) were lower than 2 µM on cervical and breast cancer cell lines, which exhibits at least a two-fold increase in sensitivity, compared to the impact of therapeutically-applied cisplatin used as a reference agent. Furthermore, tumor selectivity indices of compound **1** calculated as described above, were ranged from 0.2 to 0.7; in contrast, indices of cisplatin presented with an absolute lack of selectivity, which manifested in higher values than 1.1 on cervical and breast cancer cells. Chromatin condensation in early apoptotic cells and loss of membrane integrity in necrotic and secondary necrotic cells were visualised under a fluorescent microscope by Hoechst33258/PI staining after 24 h incubation with the test substance, which indicated a significant increase in apoptotic and necrotic cell population as well in MCF-7 and SiHa samples. To resolve limitations of this microscopic method, and for an even more detailed separation of different cell fractions such as early *vs.* late apoptotic and necrotic cells, Annexin V-Alexa488/PI fluorescent double staining was performed by flow cytometry. Significantly elevated subpopulations of late apoptotic (AnnV+/PI+) cells were detectable at ≥2 µM without greater accumulation of necrotic (AnnV–/PI+) cells on all of the utilized cell lines. In addition, a proapoptotic characteristic was confirmed by the elevated proportion of sub-G1 subpopulation in the cell cycle analysis on the utilized four malignant cell lines (MCF-7, MDA-MB-231, C33A, SiHa) as well. In all cases, a considerable arrest and accumulation of cells in the G2/M phase were observed in the expense of cells in the G0/G1 phase. A major enzyme of the execution phase, responsible for chromatin condensation and DNA fragmentation, is caspase-3; the activity of this enzyme was elevated to more than 1.5-fold after 24, 48 or 72 h exposure to 2 µM of compound **1**. Although, the caspase-3 enzyme may be activated during both the intrinsic and the extrinsic pathway of apoptosis, JC-1 staining indicated a disruption of mitochondrial membrane potential and integrity after 12 hours of exposure on breast carcinoma

cell lines and after 24 h of treatment on cervical cell lines, corroborating the intrinsic origin of apoptosis. Based on previous results and structure-activity relationships, we hypothesized that a bulky steric structure such as the 1'-4"-cyanophenyl-4'-hydroxymethyl-1'H-pyrazol-3'-yl moiety at position C-17 of the androstadiene skeleton, may diminish or prevent binding of the test compound to the androgen receptor. Lack of androgen or antiandrogen activity have been confirmed by YAS assay on a genetically modified *S. cerevisiae* strain.

In the first stage of metastasis progression, the migration of cancer cells to neighbouring tissues and the invasion through the basement membrane occurs. In the *in vitro* experimental systems, the drug candidate (**1**) significantly inhibited migration of SiHa and MCF-7 cells and invasion of highly invasive MDA-MB-231 and SiHa cells at nanomolar concentrations even after 24 h of treatment. In a 3D, co-culture CCIDs assay, compound **1** reduced the size of cell free-areas on a lymphatic endothelial monolayer underneath the MCF-7 tumor emboli by 30% after 4 h of treatment at 8 µM and showed comparable inhibition to defactinib, a potent FAK-inhibitor at lower concentrations. These values are more pronounced than inhibition by epiandrosterone, a structural analogue, in the same system.

Treatment with compound **1** decreased the expression of EGFR, CD274, and CD326 in the sensitive subpopulations of MDA-MB-231 cells, while increased level of GLUT1, MCT4 Pan-Keratins, CD66, Gal-3, and TMEM45A were observed. These data probably indicate the increased chemosensitivity and the metabolic reprogramming of cells as a compensatory mechanism, activated upon the test substance-induced oxidative stress. Interestingly, the population of CD66(a,c,e)-positive cells showed overlapping with the TMEM45A-positive cells.

Finally, antitumor properties of the examined androstadiene derivative (**1**) were tested on the 4T1 breast cancer model. After 2 weeks of intraperitoneal administration, size of developing tumors were approximately 50% relative to control samples without severe, life-threatening side effects.

In conclusion, our experimental data revealed favourable antiproliferative and antimetastatic characteristics of compound **1.** Proapoptotic properties via activation of the intrinsic pathway with moderate tumor selectivity and potent antimigratory, anti-invasive and anti-intravasative effects, without hormonal potential have been identified as part of the mechanism of action. In the light of these results, substitution of the androsta-5,16-diene framework at C-17 position with heterocyclic moieties should be considered for the design and synthesis of novel, effective antitumor agents.